Do Carbon Nanotubes Improve the Thermomechanical Properties of Benzoxazine Thermosets?

Shamil Saiev,[†] Leïla Bonnaud,[‡] Ludovic Dumas,[§,‖] Tao Zhang,[§] Philippe Dubois,[‡,§] David Beljonne,[†] and Roberto Lazzaroni*[,†,‡]

[†]Laboratory for Chemistry of Novel Materials and [§]Laboratory of Polymeric and Composite Materials, University of Mons—UMONS, Center for Innovation and Research on Materials and Polymers (CIRMAP), Place du Parc 20, 7000 Mons, Belgium

[‡]Materia Nova R&D Center, Avenue Copernic 1, Parc Initialis, 7000 Mons, Belgium

Ⓢ *Supporting Information*

ABSTRACT: Fillers are widely used to improve the thermomechanical response of polymer matrices, yet often in an unpredictable manner because the relationships between the mechanical properties of the composite material and the primary (chemical) structure of its molecular components have remained elusive so far. Here, we report on a combined theoretical and experimental study of the structural and thermomechanical properties of carbon nanotube (CNT)−reinforced polybenzoxazine resins, as prepared from two monomers that only differ by the presence of two ethyl side groups. Remarkably, while addition of CNT is found to have no impact on the glass-transition temperature (T_g) of the ethyl-decorated resin, the corresponding ethyl-free composite features a surge by ∼47 °C (50 °C) in T_g, from molecular dynamics simulations (dynamic mechanical analysis measurements), as compared to the neat resin. Through a detailed theoretical analysis, we propose a microscopic picture for the differences in the thermomechanical properties of the resins, which sheds light on the relative importance of network topology, cross-link and hydrogen-bond density, chain mobility, and free volume.

KEYWORDS: *benzoxazine thermoset, CNT nanocomposite, network topology, chain mobility, thermomechanical stability*
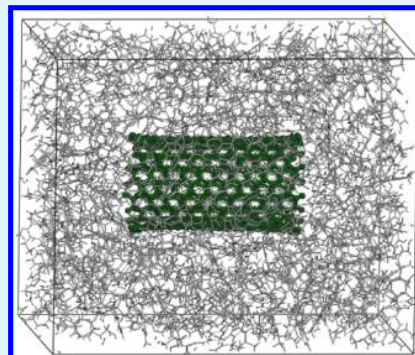
1. INTRODUCTION

Combining epoxy and phenolic resins with carbon nanotubes (CNTs) can induce a significant improvement of the electrical and thermal conductivity[1,2] and also overcome the inherent brittleness of these materials.[3] Polybenzoxazine resins are a promising class of phenolic thermosets that gained an immense interest from the scientific community since the popularization of their synthesis by Ishida.[4] The major advantages of these new thermosets are the flexibility in the molecular design, the very small volume change upon curing, the small thermal expansion, the low water uptake, and an easy thermal curing with no byproducts or catalysts required.[5] To further enhance the interest of benzoxazine resins, it is appealing to combine them with CNTs.[6−8] It has been experimentally shown that the mechanical properties of the polymer nanocomposites can be efficiently enhanced by the addition of a small percentage of CNTs.[8−10] Despite their high potential in improving the polymer composite properties, the practical applications of CNTs are hindered because of the few critical issues such as the bundle-like aggregation of CNTs within the matrix, the weak distribution/dispersion during the mixing process, and the poor interfacial binding between the CNT and the polymer, which is responsible for the efficient load transfer. In order to overcome these issues, several approaches have been developed such as chemical functionalization[11,12] and physical mixing often realized via calendaring and sonication. Even though the covalent attachment of the reactive chemical groups increases the affinity of CNTs to the polymer matrix, it also creates local defects because it alters the bond order of sp[2] carbon, leading to the decrease of overall mechanical and electrical properties.[13,14] Therefore, the noncovalent interfacial adhesion seems to be a more promising solution for the polymer reinforcement by CNTs because it can improve the interfacial interactions avoiding structural damages and maintaining the properties of CNTs.[15,16]

The choice of a given application for thermosets strongly relies on the glass-transition temperature (T_g) because it corresponds to the temperature at which the mechanical properties of any polymer drop, going from glassy to rubbery behavior. Unlike the mechanical properties that are usually enhanced by CNT incorporation, the effects of CNTs on the thermostability appear to be less clear-cut: in some cases, the presence of CNTs increases the T_g of the composites,[12,17] whereas in other cases, the T_g is decreased.[18,19] Such a complex

behavior may be due to the fact that the T_g can be affected by many physicochemical parameters such as the interfacial interaction, the degree of dispersion of the CNTs, a reduced cross-linking tendency of the resin,[19,20] different interface states between the CNTs and the polymer, or the restriction of the mobility of polymer chains, which continue to be the field of active research.[21] To disentangle all these effects, one can resort to molecular dynamics (MD) simulations that provide a molecular-scale description of the nanostructural topology and interfacial interactions between polymers and CNTs. The properties of CNT−reinforced composites were studied using MD simulations by numerous groups.[22−29] Qi et al.[26] showed that the T_g decreases in the presence of CNTs in the matrix of an aromatic copolyimide resin and also established the dependence of Young's modulus on the size of the CNTs. Khare and Khare's[27] simulations showed a dramatic drop of T_g (by 66 K) for well-dispersed CNTs in the diglycidyl ether of bisphenol A (DGEBA) epoxy resin for systems with the same degree of curing, which is attributed to the unfavorable interaction energy between the filler and the polymer, resulting in the soft and compressible interface region. Sul et al. modeled the DGEBA/4,4′-diaminodiphenyl sulfone that are both neat and composite resin structures, and the drop of the T_g by 20 K was observed.[29] The authors attributed this behavior to the interference of CNTs on the percolation of immobile domains. These studies proved the potential of MD simulations in the domain of composite materials.

In our recent work,[30] we studied by means of MD simulations the cross-linking process in two new bifunctional benzoxazine resins: phenol-p-phenylene diamine (P-pPDA)[31] and 4,4′-(p-phenylene)bis(3,4-dihydro-6-ethyl-2H-1,3 benzoxazine) (4EP-pPDA) resins (see Figure 1). Both monomers are
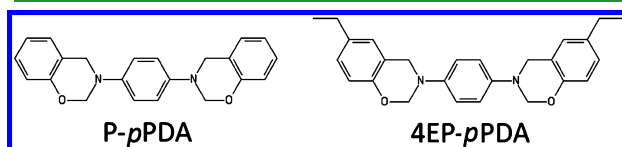
Figure 1. Molecular structure of P-pPDA and 4EP-pPDA.

based on phenol and aromatic diamines; they have an identical structure, except for additional ethyl groups attached to the external aromatic rings in 4EP-pPDA. The P-pPDA thermoset[31] has some major advantages over the classical benzoxazines, such as the commercially available bisphenol A benzoxazine (BA-a): it does not undergo any thermal degradation upon curing and shows higher thermomechanical properties with a T_g close to 220 °C; the thermomechanical stability is lower for 4EP-pPDA, its T_g being around 155 °C,

that is, similar to that of BA-a. The MD simulations allowed us (i) to construct the fully cross-linked structures for these resins, (ii) to follow the evolution of the number and type of structural defects, (iii) to calculate the cross-link density, and (iv) to evaluate their thermomechanical properties. The results are in very good agreement with the experimental data: the calculated T_g for the fully cured resins was predicted with only 1.8 and 3.2% deviation for P-pPDA and 4EP-pPDA, respectively. That study allowed us to establish a clear relationship between the T_g and the cross-link density and highlighted the role of hydrogen (H) bonds in the thermomechanical stability of polybenzoxazines.

The present study aims at a fundamental understanding of the influence of the CNTs on the thermomechanical stability of polybenzoxazines, in particular, P-pPDA and 4EP-pPDA. Experimentally, incorporation of 0.5 wt % CNT in the P-pPDA resin leads to strong increase (i.e., by nearly 50 °C) of the T_g.[6] We use atomistic simulations in order to construct and study the network topology of CNT-−reinforced P-pPDA and 4EP-pPDA polybenzoxazines and compare it with the cross-linked structures of the neat resins. We determine the molecular-scale structure of the CNT−polybenzoxazine interfaces, calculate the interaction energy between the constituents, and investigate the influence of CNTs on the T_g of these resins, in order to provide an insight on the mechanisms responsible for the thermomechanical stability of CNT−thermoset composites, which are still rather poorly understood.

2. METHODS

2.1. Simulation Details. All simulations in this work are performed using the Materials Studio 7.0 (Biovia) molecular simulation package.[32] The initial structures were prepared using Materials Studio modules and graphical interface, allowing to fill the simulation boxes with a predefined number of molecules. The prepared model structures for the simulations consist of 200 monomer molecules (P-pPDA or 4EP-pPDA) placed into 4.5 × 4.5 × 5.5 nm³ simulation cells under three-dimensional periodic boundary conditions. The influence of the CNTs is modeled by inserting in the center of the simulation box a short single-walled carbon armchair nanotube segment of chirality (10, 10), having a length of 2.46 nm and a diameter of 1.36 nm (see Figure 2, left). Although the interfacial and thermomechanical properties of polymer−CNT systems show some dependence on the CNT diameter for values below 1−1.3 nm, these level off for larger diameters.[33−35] The use of (10, 10) CNTs thus appears to offer the best compromise between robustness and accuracy of the results and computational cost. The interatomic carbon bond length is set at 0.142 nm.[36] The final monomer nanocomposite structures correspond to a CNT weight content of 7.7 and 6.6 wt % for P-pPDA and 4EP-pPDA, respectively. Twenty different initial structures are generated for each compound, and only the five structures with the lowest potential energy are used for further NPT MD simulations at 298 K
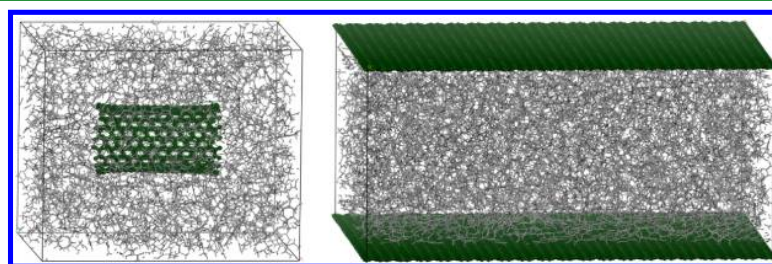
Figure 2. Snapshot of a CNT segment inserted in a polybenzoxazine box (left) and polybenzoxazine sandwiched between two graphene sheets (right).
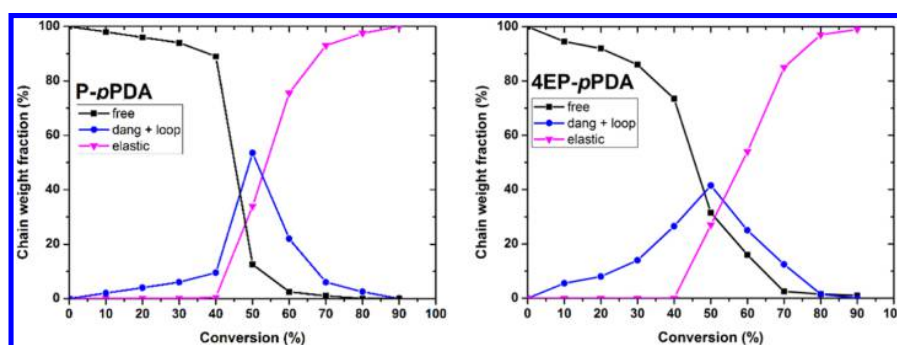
Figure 3. Fractions of free, dangling, loop, and elastic chains as a function of the conversion rate for P-*p*PDA (left) and 4EP-*p*PDA (right) cross-linked in the presence of CNTs.

and at 1 atm. Because the (10,10) CNT may not be fully representative of the actual CNTs used in reinforced polymers [multiwalled CNTs (MWCNTs) with diameter $\geq$ 10 nm and length $\geq$ 1 μm], we also consider model interfaces between polybenzoxazines and graphene sheets, that is, the extreme case of carbon nanostructures with a small surface curvature. The graphene-containing structures are prepared in the same manner as the CNT structures, using a $6.0 \times 5.7 \times 3.0$ nm^3 simulation box. In practice, the benzoxazine medium is sandwiched between two rigid graphene sheets (Figure 2, right).

The total potential energy of the system is described by the optimized version of Dreiding force field,[37] adapted to represent at best the behavior of benzoxazines (see the Supporting Information). The atomic charges are calculated using the Gasteiger iterative method.[38] The van der Waals interactions are explicitly calculated using the Lennard-Jones (12-6) potential function. For the electrostatic interactions, a group-based summation is used, which effectively reduces the energy fluctuations and the computational effort compared to other methods such as Ewald or particle−particle and particle-mesh summations. For these two interactions, the cutoff distance is set at 1.2 nm. In NPT calculations (the constant number of particles, pressure, and temperature), the Parrinello−Rahman barostat is used for the pressure control (always at the atmospheric pressure); the high number of degrees of freedom in this barostat allows the system to relax more naturally. The temperature is controlled by means of the Nosé−Hoover−Langevin thermostat with a Q ratio of 0.01.[39]

The cross-linked networks considered in this study are constructed using the cyclic polymerization atomistic model with conducted multistep topology relaxation:[30] (i) the prepared structures undergo a pre-equilibrium step in the NPT ensemble first for 0.5 ns at 800 K and then for 2 ns at 300 K under atmospheric pressure and (ii) the cross-linking process is then initiated. It is based on a ring-opening mechanism: the monomers bind through the Mannich bridge between the nitrogen atom and the aromatic ring.[40,41] Here, we consider only the reaction on the ortho position because the probability of reaction on this site is much higher than on the para and meta positions.[42] A distance-based criterion ranging from 0.4 to 0.8 nm is used to trigger the formation of new bonds between the reactive atoms. When the distance criterion is satisfied, the oxazine cycle is opened by breaking the O−C bond and a new covalent bond is created. After formation of all possible bonds, the system undergoes a multistep relaxation−perturbation procedure using the NVT−NPT dynamics, and then attempts to find more atoms satisfying the bond-creation condition are undertaken. The conversion rate of polymerization is defined as the ratio between the reacted atoms and the total number of reactive atoms initially present in the structure. The cross-linking process proceeds until the predefined conversion limit is reached, which is set here at 90%; (iii) the structural characteristics of the network are calculated through the monitoring of the macromolecular parameters during cross-linking: the number-/weight-average molar masses, M_n and M_w, respectively, and the reduced weight-average degree of polymerization (RDP), which defines the gel point and the gel fraction.[43]

In the analysis of the system morphology, all the molecules in the sol phase, that is, monomers and oligomers, are considered as "free chains". In contrast, the gel fraction consists of elastically active cross-links and elastically active chains with three or more and two paths, leading to the infinite network, respectively. The chains having only one path leading to the gel, such as dangling and loop chains, are not involved in the elastic response of the cross-linked networks and are considered as structural defects. The structural defects such as dangling−loop chains and elastically active chains are counted by means of a home-made algorithm described in our previous work.[30]

In the MD simulations, the thermal and volumetric properties of the cross-linked networks are assessed by a stepwise temperature excursion going from high to low temperatures. First, the cross-linked structures are equilibrated at 850 K for 1 ns in the NPT ensemble, in order to release all the constraints created during the cross-linking process. Thereafter, the equilibrated structures are cooled down stepwise from 850 to 50 K with a relaxation period of 400 ps between two steps. We have shown that for these benzoxazine thermosets, such a cooling rate is sufficiently small for the structures to reach equilibrium.[30] The temperature, volume, valence, and nonbonded energies are averaged and stored for further analysis. The T_g is defined as the intersection of the linear density−temperature curves of the glassy and rubbery states.

2.2. Experimental Details. Experimentally, the incorporation and dispersion of MWCNTs in the benzoxazine monomers are obtained by ultrasonication in solution for 10 min with a Branson S-50D apparatus (200 W, 20 kHz and 13 mm ultrasonic probe). The thermomechanical properties are studied with dynamic mechanical thermal analysis (DMA 2980 Dynamical Mechanical Analyzer from TA Instruments). The measurements are realized in a dual cantilever configuration with a length of 35 mm, operating at a frequency of 1 Hz, from 25 to 370 °C at a heating rate of 3 °C/min, with a displacement of 18 μm corresponding to a strain of 0.043%.[6]

3. RESULTS AND DISCUSSION

It is assumed that the T_g of thermoset polymers is strongly dependent on the cross-link density because it restricts the segmental mobility of chains.[44] The free volume is also an important factor, leading to a partial reduction in intermolecular cooperativity between the chains.[45] Therefore, the enhancement of the T_g for CNT−reinforced thermosets may be attributed not only to several factors such as the increase of the local cross-link density, because of the higher concentration of monomers at the interface, but also to strong CNT−filler interactions, which lead to the decrease of the interfacial molecular mobility.[12,46,47] Consistently, for a given polymer, a decrease of thermomechanical stability can be associated with the decrease of the cross-linking tendency of the resin[48] and increase of the free volume and/or poor CNT−filler
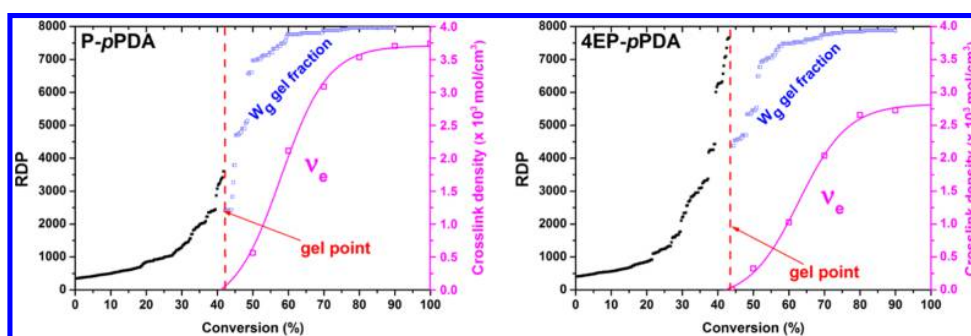
Figure 4. Evolution of the number-weight average molecular weight (black dots), the cross-link density (pink dots and curve), and the gel fraction (blue dots) as a function of the conversion rate for P-*p*PDA and 4EP-*p*PDA in the presence of CNTs.

interactions.[27] Furthermore, the presence of CNTs could induce the formation of structural defects in the network, which could also promote additional chain mobility. In the current MD investigation, we study the connection between these structural features and the thermomechanical stability of the benzoxazine−CNT composites.

3.1. Network Topology. Figure 3 portrays the weight percent evolution of free, dangling, loop, and elastic chains as a function of the conversion. In the early stages of the cross-linking process, the number of free chains decreases because of the appearance in the medium of dimers and oligomers, which are counted as one chain. Free chains disappear completely at high conversion rates for both P-*p*PDA and 4EP-*p*PDA. The first appearance of the elastic chains corresponds to the gelation point, which is located between 40 and 50% of conversion for both resins. At the gel point, the number of dangling and loop chains is maximal and decreases progressively until complete disappearance at 90% conversion rate. At high conversion degrees, the free, dangling, and loop chains are consumed and the fully cross-linked resins are considered to be completely elastic. This behavior is very similar to what we observed previously in the cross-linking of both neat resins,[30] indicating that the incorporation of CNTs does not affect the formation and the final topology of the network in these polybenzoxazines.

The cross-link density v_e is extensively used for the characterization of cross-linked polymers because it can be experimentally estimated by measuring the equilibrium modulus in the rubbery state.[49] However, it is experimentally impossible to quantify the number of structural defects (dangling and loop chains) in the thermosets, which in practice leads to the overestimation of the cross-link density. From the MD simulations, it is possible to calculate the exact value of v_e by taking specifically into account the number of dangling and loop chains. The MD simulations can therefore be used as a tool that, combined with the experimental results, is able to refine the experimental prediction models.[50]

It was already pointed out that the cross-link density v_e, the gel fraction W_g, and the maxima of RDP are the quantities that define the gelation during the polymerization process. Figure 4 shows the evolution of these structural characteristics as a function of the conversion rate. The gelation points calculated from the RDP curves are 41.5 ± 3.5 and 43.2 ± 3.2% for P-*p*PDA and 4EP-*p*PDA, respectively; this is consistent with the rapid increase of W_g at the gel point and the evolution of the cross-link density. These values are very close to those obtained previously on the neat resins.[30] The calculations also show that the (free) volume of the polybenzoxazine

component in the CNT−resin system is very close to the situation in the neat resins (see the Supporting Information). Because there is no significant change in the volume and the initial number of the benzoxazine molecules is the same for both neat resins and the CNT−resin structures, we can conclude that the cross-link density of the benzoxazine nanocomposites does not change upon incorporation of CNTs. This further indicates that the presence of CNTs in the benzoxazine matrices does not influence significantly the structural properties of the polymer network.

3.2. Glass Transition and Thermal Expansion. The calculated T_g values for CNT-containing P-*p*PDA and 4EP-*p*PDA resins are represented in Figure 5 as a function of the conversion rate and compared with the T_g of the neat resins.[30] For neat P-*p*PDA, the T_g varies from 37 °C in the monomer up to 216 °C in the fully cross-linked resin. This closely agrees with the corresponding experimental values of 45 and 220 °C, before and after reticulation, respectively.[6] The neat 4EP-*p*PDA resin is much less thermomechanically stable, with the
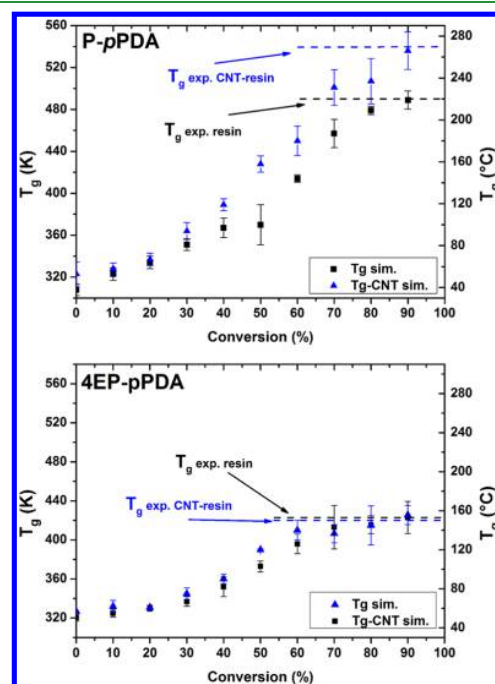
Figure 5. T_g as a function of the conversion rate for P-*p*PDA (top) and 4EP-*p*PDA (bottom) and for the neat resins (black marks) and the CNT−resin systems (blue marks).

calculated T_g going from 47 °C (monomer) to 150 °C (fully cross-linked), which is also in very good agreement with the experimental value for the fully cured resin: 155 °C. As it was shown in our previous work, this thermomechanical stability difference between the two polybenzoxazines is directly related to the combined influence of the cross-link density (3.6×10^{-3} mol cm^{-3} for P-pPDA vs 2.75×10^{-3} mol cm^{-3} for 4EP-pPDA) and the H-bond density (2.6×10^{-3} mol cm^{-3} in P-pPDA vs 1.9×10^{-3} mol cm^{-3} in 4EP-pPDA).

In the presence of CNTs, the T_g of the P-pPDA composite shifts toward higher temperatures. Above gelation, the T_g surges significantly with respect to the neat resin. For the fully cross-linked system, the T_g increase is as high as 47 °C; experimentally, the T_g of the P-pPDA−CNT composite is raised by nearly 50 °C with 0.5 wt % of CNT.[6] In contrast, the simulations show that the presence of CNTs has no influence on the T_g of the 4EP-pPDA−CNT composites, whatever the conversion rate. This result is experimentally verified: the T_g of the fully cured 4EP-pPDA composites is found to be in the same range as that of the neat resin (see Figure 5, bottom). The presence of CNTs thus has a different influence on the thermomechanical stability of P-pPDA and 4EP-pPDA composites, despite the similarity in their molecular structures. Because we have shown that the cross-link density and the free volume are not modified by the incorporation of CNTs, it seems reasonable to hypothesize that the difference in thermomechanical stability induced by the CNTs is related to the interfacial interactions and the mobility of the polymer chains.

3.3. Polymer−CNT Interactions.

In this section, we use MD simulations to investigate model systems for the resin−carbon interfaces in order to get a general understanding of the behavior and the nature of the interactions of benzoxazine molecules on a sp^2-hybridized carbon surface. At the local scale considered here, the surface of a realistic MWCNT (i.e., with a diameter of around 10 nm) can be reasonably viewed as almost flat and be represented by a graphene plane. The validity of such an approximation has been established in the modeling studies of other polymer−CNT nanocomposites.[51] This assumption allows a more detailed investigation of the nature and strength of the interactions at the polymer−CNT interface. To gain an insight on the adsorption of the benzoxazines on the CNT surface, we define normal vectors to each aromatic ring of the monomers (P1, P2, and P3 in Figure 6) in order to keep track of the ring orientation during
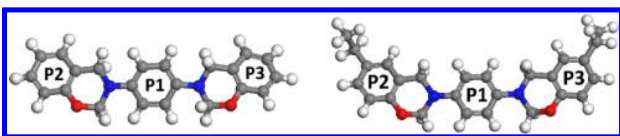
Figure 6. P-pPDA (left) and 4EP-pPDA (right) monomers with the aromatic rings labeled.

the MD simulations. In practice, we follow the angle between those normal vectors and the normal vector to the graphene plane during the simulations.

The MD simulations were conducted at 300 K for 1 ns. Figure 7 shows the evolution of the angle between the normal vector to the graphene surface and those normal to P1, P2, and P3 as a function of time. All the angles rapidly tend to zero, indicating that the molecules readily adsorb flat on the surface as a result of π−π interactions with graphene (see typical

snapshots in Figure 7, bottom). The adhesion energies of isolated molecules on graphene are 338 and 352 mJ/m^2 for P-pPDA and 4EP-pPDA, respectively. The higher adhesion energy of 4EP-pPDA is related to the presence of additional ethyl groups, which provide CH−π interactions in addition to the π−π interactions.

As the second step in this part of the study, we investigate the formation of the cross-linked resins between two graphene planes (see Figure 2, right). The cross-linking algorithm is used in the same manner as that in the CNT−polymer systems. It is proposed in the literature that interfacial constraints play a vital role in the T_g shift; according to that mechanism, a few nanometer thick, highly restrained layer develops near the surface of the fillers.[47] The molecular chains in the interfacial region are under constraint because of the additional interactions between the filler and the polymer matrix, which leads to the higher T_g. However, the incorporation of the filler into the polymer also increases the free volume, which favors the large-scale molecular motion of the chains. Therefore, there usually exists an optimal concentration of the filler corresponding to the best balance between the two effects.

The polymer chain interfacial arrangement with respect to the surface can be estimated through the calculation of the density profiles as a function of the distance from the graphene layers. These density profiles are shown in Figure 8 for P-pPDA and 4EP-pPDA before and after cross-linking. We can clearly identify the interface region, which is about 1 nm thick for both resins. The highest peaks in the profile correspond to the first layer of monomers that lie flat on the surfaces. A second, less intense, peak corresponds to the formation of the second layer of monomers over the first one. Further away from the surface, the density reaches the bulk value, corresponding to the end of the interfacial region. For the fully cross-linked resins, the layering at the surface slightly decreases because of the steric constraints induced by the bonding between the monomer units. Nevertheless, the presence of a denser layer in contact with the carbon surface can still be identified.

The comparison between the two benzoxazines indicates that the layering of the chains on the carbon surface is higher for P-pPDA for both the monomer and the fully cross-linked structure. This is confirmed by the adhesion energy values presented in Table 1. For isolated molecules, the adhesion energy is larger for 4EP-pPDA than for P-pPDA because of the larger molecular footprint. In contrast, the interaction of the full 4EP-pPDA resin with the carbon surface is weaker than in the corresponding P-pPDA system. This is due to the presence of ethyl groups in 4EP-pPDA, which reduces the density of π−π interactions at the interface. For both uncured and cured structures, the energy difference between the two benzoxazines is equal to $\Delta E_{uncured} \approx 27$ mJ/m^2 and $\Delta E_{cured} \approx 20$ mJ/m^2.

The effects of the interfacial interaction energy on the stabilization of the polymer are complex, yet have a crucial role on the physics of polymers in nanocomposites. It was concluded from various studies that the T_g in the interface region between the polymer and a substrate is strongly dependent on the nature of interfacial interactions.[52−54] Particularly, because the interface region in nanocomposites corresponds to a larger volume fraction compared to that in traditional composites (because of the finer dispersion of the filler), the nanocomposites are expected to be more sensitive to the nanofiller−polymer interface. However, one must also take into account other parameters such as the free volume, the
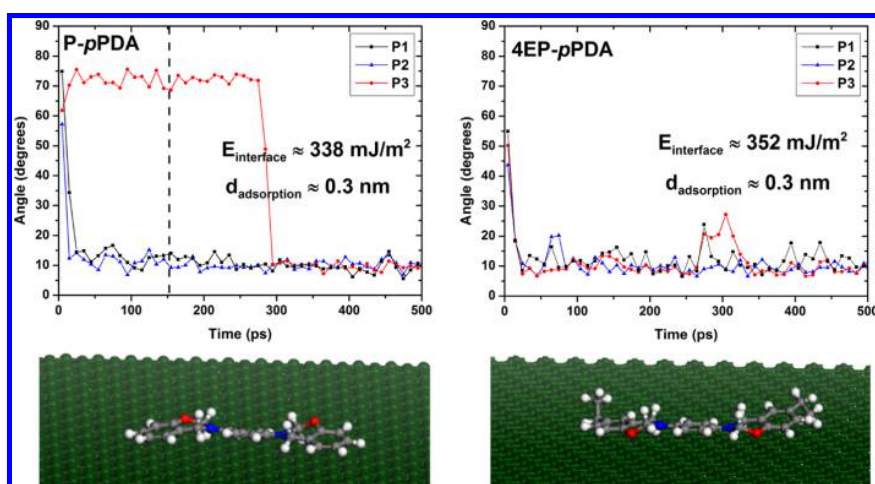
Figure 7. (top) Evolution of the angle distribution between the normal vectors to the graphene plane and the aromatic rings for P-*p*PDA and 4EP-*p*PDA during 1 ns long MD simulations; (bottom) snapshots illustrating the conformation of adsorbed P-*p*PDA and 4EP-*p*PDA monomers.
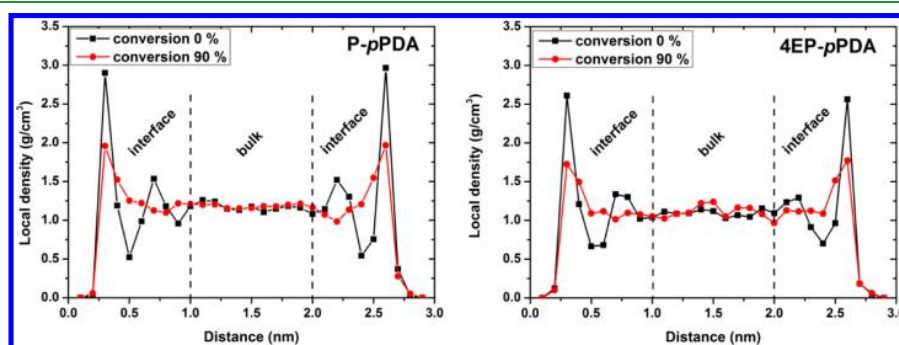
Figure 8. Local density of the P-*p*PDA (left) and 4EP-*p*PDA (right) resins as a function of the distance between two graphene planes: uncured (black squares) vs cured systems (red dots).

Table 1. Adhesion Energy for P-*p*PDA and 4EP-*p*PDA Adsorbed on Graphene at 0 and 90% Conversion (mJ/m²)

	P-*p*PDA	4EP-*p*PDA
conversion 0%	482.7 ± 4.4	455.8 ± 3.0
conversion 90%	400.3 ± 2.3	380.3 ± 4.7

cross-link density, and the mobility of the chains. Here, the interaction energy for uncured P-*p*PDA and 4EP-*p*PDA systems has higher values compared to that for cured structures; however, there is no noticeable effect on the T_g of the uncured nanocomposites (see Figure 5). For P-*p*PDA–CNT, the T_g increase with respect to the neat resin becomes significant only after the gel point, which corresponds to the point where the largest P-*p*PDA fragment becomes infinite.

One may conclude that below the gelation, the CNTs have only a short-range impact, that is, on the closest monomer molecules; it is only when the gel point is reached that the effect of the nanotubes propagates through the whole polymer network.

3.4. H Bonds and Chain Mobility. The role of the H bonds is decisive for the thermomechanical stability of benzoxazine thermosets as the T_g difference between P-*p*PDA and 4EP-*p*PDA resins is partially due to the density of the H bonds.[30] To assess whether the effect of the CNTs on the T_g can originate from differences in the density of H bonds, that parameter was calculated for fully cured benzoxazine structures. The analysis shows that there is a slight increase in the density of H bonds for the P-*p*PDA–CNT composite compared to that for the neat resin, going from 2.60 to 2.64 ×

Table 2. Density of H Bonds and Increase of Torsional Energy between Glassy and Rubbery States for P-*p*PDA and 4EP-*p*PDA Neat Resins and Nanocomposites at 90% Conversion[a]

	P-*p*PDA	P-*p*PDA CNT	4EP-*p*PDA	4EP-*p*PDA CNT
H bonds (×10⁻³ mol cm⁻³)	2.60 ± 0.06[30]	2.64 ± 0.02	1.90 ± 0.06[30]	1.81 ± 0.09
ΔH bonds (×10⁻³ mol cm⁻³)		0.04		−0.09
Δenergy torsion (kcal/mol)	2590 ± 45	2621 ± 36	2923 ± 18	3129 ± 41
Δenergy torsion$_{comp-resin}$		+31		+206

[a](1) First line corresponds to the structural H-bond density, and the second line represents the difference between the neat resin and the nanocomposite; (2) third line stands for the torsional energy difference between glassy and rubbery states (100 and 700 K), whereas fourth line represents the difference between the neat resin and the nanocomposite.

10^{-3} mol cm^{-3}; in contrast, there is a small decrease in the H-bond density in the case of 4EP-pPDA, from 1.91×10^{-3} mol cm^{-3} in the neat cross-linked resin to 1.81×10^{-3} mol cm^{-3} in the composite. Although these results show the right trend compared to the observed T_g shift, the change in the H-bond density is so small that this factor can be considered to play only a minor role.

Next, we examine the mobility of polybenzoxazine chains, by evaluating the torsional energy difference $\Delta E_{torsion}$ between the structures in the glassy and the rubbery states. Elder et al.[55] demonstrated the existence of twisting motions of different molecular segments, which were quantified from the examination of torsion angles. In practice, we extract the torsional energy contribution from the total potential energy for MD simulations of the cross-linked resins at 100 and 700 K and define $\Delta E_{torsion}$ as $E_{torsion-700K} - E_{torsion-100K}$. The value of $\Delta E_{torsion}$ reflects the increase in chain mobility upon the thermal excursion; it is equal to 2590 ± 45 and 2923 ± 18 kcal/mol for P-pPDA and 4EP-pPDA neat resins, respectively (see Table 2). In the case of the nanocomposites, $\Delta E_{torsion}$ remains basically unchanged for P-pPDA (the increase of 31 kcal/mol is within the error bar of the measurement), whereas a significant increase of 200 kcal/mol is found for 4EP-pPDA. This indicates that the presence of CNTs in the P-pPDA−CNT structure does not significantly affect the chain mobility and as a consequence has no effect on the T_g. In contrast, the chain mobility is noticeably higher for the 4EP-pPDA−CNT composite compared to that for the neat resin. This behavior is commonly observed in polymer thin films and nanocomposites, whose confinement usually induces the increase of chain mobility and decrease of the T_g.[56,57] Roth and Dutcher[58] demonstrated that the segmental chain mobility, which differs from the bulk chain mobility, can be enhanced in very thin polymer films, leading to a significant reduction in the T_g. We suggest that the calculated additional chain mobility in the 4EP-pPDA nanocomposite most probably counterbalances the effect of interfacial interactions, resulting in the invariance of the T_g in the 4EP-pPDA−CNT system.

4. CONCLUSIONS

In this work, we studied the influence of the CNTs on the thermomechanical stability of P-pPDA and 4EP-pPDA polybenzoxazines using molecular modeling. The T_g of these nanocomposites was calculated for different cross-link densities and compared to the values obtained for the neat resins. Experimentally, the T_g of these materials responds differently to the presence of CNTs in the network: the T_g of the P-pPDA−CNT composite shifts by nearly 50 °C toward higher temperatures, whereas it remains invariant for the 4EP-pPDA−CNT composite. The simulations quantitatively account for those observations, and a detailed analysis of the theoretical data has been performed to shed light on the origin of the differences between these two nanocomposites.

The study of the network topology allowed us to quantify structural characteristics such as the gelation point, reduced RDP, free volume, and cross-link and H-bond density, along with the number of dangling and loop chains representing the structural defects. The polymer−CNT interface was also investigated by studying the interactions of the monomers and cross-linked polymers with a model carbon surface.

The results show that the presence of CNTs has no effect on the overall structuration of the fully cured polybenzoxazines in terms of cross-link density and structural defects. Similarly, the H-bond density is not found to vary significantly in the presence of the CNTs. We thus hypothesized that the most important role on the T_g behavior in these systems can be attributed to the balance between the chain mobility and the polybenzoxazine−CNT interaction energy: the filler−polymer interactions are favorable in both nanocomposites, which is expected to raise the T_g. However, in 4EP-pPDA, the presence of the CNTs also leads to an increase in the chain mobility, which is expected to decrease the T_g and counterbalance the effect of the interface interactions. As a result, a net increase of the T_g is observed only in P-pPDA−CNT composites.

The methodology presented in this work, based on the simulation and characterization of the structural and thermomechanical properties of the cross-linked systems, along with the detailed analysis of the polymer−nanofiller interfaces, thus provides information on the mechanisms ruling the glass transition in nanocomposites and could be extended to other families of thermosets.

■ ASSOCIATED CONTENT

ⓢ Supporting Information

The Supporting Information is available free of charge on the ACS Publications website at DOI: 10.1021/acsami.8b08473.

> Volume and H-bond density change of the resins in the presence of CNT and optimization of the Dreiding force field for benzoxazine molecules (PDF)
> Uncured and fully cured polymer−CNT structures (ZIP)

■ AUTHOR INFORMATION

Corresponding Author
*E-mail: roberto.lazzaroni@umons.ac.be.

ORCID ⓞ
Roberto Lazzaroni: 0000-0002-6334-4068

Present Address
∥Huntsman Advanced Materials, Klybeckstrasse 200, 4057 Basel, Switzerland.

Author Contributions
The manuscript was written through contributions of all authors. All authors have given approval to the final version of the manuscript.

Notes
The authors declare no competing financial interest.

■ ACKNOWLEDGMENTS

■ REFERENCES

(1) Thostenson, E. T.; Chou, T.-W. Processing-Structure-Multi-Functional Property Relationship in Carbon Nanotube/Epoxy Composites. *Carbon* **2006**, *44*, 3022−3029.

(2) Yang, Y.; Gupta, M. C.; Zalameda, J. N.; Winfree, W. P. Dispersion Behaviour, Thermal and Electrical Conductivities of

Carbon Nanotube-Polystyrene Nanocomposites. *Micro Nano Lett.* **2008**, 3, 35−40.

(3) Thostenson, E. T.; Chou, T.-W. Aligned Multi-Walled Carbon Nanotube-Reinforced Composites: Processing and Mechanical Characterization. *J. Phys. D: Appl. Phys.* **2002**, 35, L77.

(4) Ning, X.; Ishida, H. Phenolic Materials via Ring-Opening Polymerization: Synthesis and Characterization of Bisphenol-A Based Benzoxazines and Their Polymers. *J. Polym. Sci., Part A: Polym. Chem.* **1994**, 32, 1121−1129.

(5) Ghosh, N. N.; Kiskan, B.; Yagci, Y. Polybenzoxazines-New High Performance Thermosetting Resins: Synthesis and Properties. *Prog. Polym. Sci.* **2007**, 32, 1344−1391.

(6) Dumas, L.; Bonnaud, L.; Olivier, M.; Poorteman, M.; Dubois, P. High Performance Benzoxazine/CNT Nanohybrid Network-An Easy and Scalable Way to Combine Attractive Properties. *Eur. Polym. J.* **2014**, 58, 218−225.

(7) Zúñiga, C.; Bonnaud, L.; Lligadas, G.; Ronda, J. C.; Galià, M.; Cádiz, V.; Dubois, P. Convenient and Solventless Preparation of Pure Carbon Nanotube/Polybenzoxazine Nanocomposites with Low Percolation Threshold and Improved Thermal and Fire Properties. *J. Mater. Chem. A* **2014**, 2, 6814−6822.

(8) Dumas, L.; Bonnaud, L.; Dubois, P. Polybenzoxazine Nanocomposites: Case Study of Carbon Nanotubes. *Advanced and Emerging Polybenzoxazine Science and Technology*; Elsevier, 2017; pp 767−800.

(9) Li, X.; Gao, H.; Scrivens, W. A.; Fei, D.; Xu, X.; Sutton, M. A.; Reynolds, A. P.; Myrick, M. L. Nanomechanical Characterization of Single-Walled Carbon Nanotube Reinforced Epoxy Composites. *Nanotechnology* **2004**, 15, 1416.

(10) Sen, R.; Zhao, B.; Perea, D.; Itkis, M. E.; Hu, H.; Love, J.; Bekyarova, E.; Haddon, R. C. Preparation of Single-Walled Carbon Nanotube Reinforced Polystyrene and Polyurethane Nanofibers and Membranes by Electrospinning. *Nano Lett.* **2004**, 4, 459−464.

(11) Bal, S.; Samal, S. S. Carbon Nanotube Reinforced Polymer Composites-A State of the Art. *Bull. Mater. Sci.* **2007**, 30, 379.

(12) Gojny, F. H.; Schulte, K. Functionalisation Effect on the Thermo-Mechanical Behaviour of Multi-Wall Carbon Nanotube/ Epoxy-Composites. *Compos. Sci. Technol.* **2004**, 64, 2303−2308.

(13) Coto, B.; Antia, I.; Blanco, M.; Martinez-de-Arenaza, I.; Meaurio, E.; Barriga, J.; Sarasua, J.-R. Molecular Dynamics Study of the Influence of Functionalization on the Elastic Properties of Single and Multiwall Carbon Nanotubes. *Comput. Mater. Sci.* **2011**, 50, 3417−3424.

(14) Buffa, F.; Abraham, G. A.; Grady, B. P.; Resasco, D. Effect of Nanotube Functionalization on the Properties of Single-Walled Carbon Nanotube/Polyurethane Composites. *J. Polym. Sci., Part B: Polym. Phys.* **2007**, 45, 490−501.

(15) Chen, J.; Liu, H.; Weimer, W. A.; Halls, M. D.; Waldeck, D. H.; Walker, G. C. Noncovalent Engineering of Carbon Nanotube Surfaces by Rigid, Functional Conjugated Polymers. *J. Am. Chem. Soc.* **2002**, 124, 9034−9035.

(16) Star, A.; Liu, Y.; Grant, K.; Ridvan, L.; Stoddart, J. F.; Steuerman, D. W.; Diehl, M. R.; Boukai, A.; Heath, J. R. Noncovalent Side-Wall Functionalization of Single-Walled Carbon Nanotubes. *Macromolecules* **2003**, 36, 553−560.

(17) Gong, X.; Liu, J.; Baskaran, S.; Voise, R. D.; Young, J. S. Surfactant-Assisted Processing of Carbon Nanotube/Polymer Composites. *Chem. Mater.* **2000**, 12, 1049−1052.

(18) Liao, Y.-H.; Marietta-Tondin, O.; Liang, Z.; Zhang, C.; Wang, B. Investigation of the Dispersion Process of SWNTs/SC-15 Epoxy Resin Nanocomposites. *Mater. Sci. Eng. A* **2004**, 385, 175−181.

(19) Tao, K.; Yang, S.; Grunlan, J. C.; Kim, Y.-S.; Dang, B.; Deng, Y.; Thomas, R. L.; Wilson, B. L.; Wei, X. Effects of Carbon Nanotube Fillers on the Curing Processes of Epoxy Resin-Based Composites. *J. Appl. Polym. Sci.* **2006**, 102, 5248−5254.

(20) Wang, S.; Liang, Z.; Gonnet, P.; Liao, Y.-H.; Wang, B.; Zhang, C. Effect of Nanotube Functionalization on the Coefficient of Thermal Expansion of Nanocomposites. *Adv. Funct. Mater.* **2007**, 17, 87−92.

(21) Grady, B. P. Effects of Carbon Nanotubes on Polymer Physics. *J. Polym. Sci., Part B: Polym. Phys.* **2012**, 50, 591−623.

(22) Khare, K. S.; Khabaz, F.; Khare, R. Effect of Carbon Nanotube Functionalization on Mechanical and Thermal Properties of Cross-linked Epoxy-Carbon Nanotube Nanocomposites: Role of Strengthening the Interfacial Interactions. *ACS Appl. Mater. Interfaces* **2014**, 6, 6098−6110.

(23) Gao, Y.; Müller-Plathe, F. Molecular Dynamics Study on the Thermal Conductivity of the End-grafted Carbon Nanotubes Filled Polyamide-6.6 Nanocomposites. *J. Phys. Chem. C* **2018**, 122, 1412−1421.

(24) Demir, B.; Henderson, L. C.; Walsh, T. R. Design Rules for Enhanced Interfacial Shear Response in Functionalized Carbon Fiber Epoxy Composites. *ACS Appl. Mater. Interfaces* **2017**, 9, 11846−11857.

(25) Kropka, J. M.; Pryamitsyn, V.; Ganesan, V. Relation Between Glass Transition Temperatures in Polymer Nanocomposites and Polymer Thin Films. *Phys. Rev. Lett.* **2008**, 101, 075702.

(26) Qi, D.; Hinkley, J.; He, G. Molecular Dynamics Simulation of Thermal and Mechanical Properties of Polyimide-Carbon-Nanotube Composites. *Modell. Simul. Mater. Sci. Eng.* **2005**, 13, 493.

(27) Khare, K. S.; Khare, R. Effect of Carbon Nanotube Dispersion on Glass Transition in Cross-linked Epoxy-Carbon Nanotube Nanocomposites: Role of Interfacial Interactions. *J. Phys. Chem. B* **2013**, 117, 7444−7454.

(28) Zhu, R.; Pan, E.; Roy, A. K. Molecular Dynamics Study of the Stress-Strain Behavior of Carbon-Nanotube Reinforced Epon 862 Composites. *Mater. Sci. Eng. A* **2007**, 447, 51−57.

(29) Sul, J.-H.; Prusty, B. G.; Kelly, D. W. Application of Molecular Dynamics to Evaluate the Design Performance of Low Aspect Ratio Carbon Nanotubes in Fibre Reinforced Polymer Resin. *Composites, Part A* **2014**, 65, 64−72.

(30) Saiev, S.; Bonnaud, L.; Dubois, P.; Beljonne, D.; Lazzaroni, R. Modeling the Formation and Thermomechanical Properties of Polybenzoxazine Thermosets. *Polym. Chem.* **2017**, 8, 5988−5999.

(31) Dumas, L.; Bonnaud, L.; Olivier, M.; Poorteman, M.; Dubois, P. Facile Preparation of a Novel High Performance Benzoxazine-CNT Based Nano-Hybrid Network Exhibiting Outstanding Thermo-Mechanical Properties. *Chem. Commun.* **2013**, 49, 9543−9545.

(32) *Materials Studio* R2; Dassault Systèmes BIOVIA: San Diego, 2017.

(33) Coto, B.; Antia, I.; Barriga, J.; Blanco, M.; Sarasua, J.-R. Influence of the Geometrical Properties of the Carbon Nanotubes on the Interfacial Behavior of Epoxy/CNT Composites: a Molecular Modelling Approach. *Comput. Mater. Sci.* **2013**, 79, 99−104.

(34) Yang, M.; Koutsos, V.; Zaiser, M. Interactions Between Polymers and Carbon Nanotubes: a Molecular Dynamics Study. *J. Phys. Chem. B* **2005**, 109, 10009−10014.

(35) Malagù, M.; Lyulin, A.; Benvenuti, E.; Simone, A. A Molecular-Dynamics Study of Size and Chirality Effects on Glass-Transition Temperature and Ordering in Carbon Nanotube-Polymer Composites. *Macromol. Theory Simul.* **2016**, 25, 571−581.

(36) Ciraci, S.; Dag, S.; Yildirim, T.; Gülseren, O.; Senger, R. T. Functionalized Carbon Nanotubes and Device Applications. *J. Phys.: Condens. Matter* **2004**, 16, R901.

(37) Mayo, S. L.; Olafson, B. D.; Goddard, W. A. DREIDING: a Generic Force Field for Molecular Simulations. *J. Phys. Chem.* **1990**, 94, 8897−8909.

(38) Gasteiger, J.; Marsili, M. Iterative Partial Equalization of Orbital Electronegativity−a Rapid Access to Atomic Charges. *Tetrahedron* **1980**, 36, 3219−3228.

(39) Samoletov, A. A.; Dettmann, C. P.; Chaplain, M. A. J. Thermostats for "Slow" Configurational Modes. *J. Stat. Phys.* **2007**, 128, 1321−1336.

(40) Burke, W. J.; Glennie, E. L. M.; Weatherbee, C. Condensation of Halophenols with Formaldehyde and Primary Amines1. *J. Org. Chem.* **1964**, 29, 909−912.

(41) Burke, W. J.; Bishop, J. L.; Glennie, E. L. M.; Bauer, W. N., Jr. A New Aminoalkylation Reaction. Condensation of Phenols with Dihydro-1, 3-Aroxazines. *J. Org. Chem.* **1965**, *30*, 3423−3427.

(42) Ishida, H.; Sanders, D. P. Regioselectivity of the Ring-Opening Polymerization of Monofunctional Alkyl-Substituted Aromatic Amine-Based Benzoxazines. *Polymer* **2001**, *42*, 3115−3125.

(43) Shy, L. Y.; Leung, Y. K.; Eichinger, B. E. Critical Exponents for Off-Lattice Gelation of Polymer Chains. *Macromolecules* **1985**, *18*, 983−986.

(44) Stutz, H.; Illers, K.-H.; Mertes, J. A generalized Theory for the Glass Transition Temperature of Crosslinked and Uncrosslinked Polymers. *J. Polym. Sci., Part B: Polym. Phys.* **1990**, *28*, 1483−1498.

(45) Bershtein, V. A.; Egorova, L. M.; Yakushev, P. N.; Pissis, P.; Sysel, P.; Brozova, L. Molecular Dynamics in Nanostructured Polyimide-Silica Hybrid Materials and Their Thermal Stability. *J. Polym. Sci., Part B: Polym. Phys.* **2002**, *40*, 1056−1069.

(46) Ganguli, S.; Aglan, H.; Dennig, P.; Irvin, G. Effect of Loading and Surface Modification of MWCNTs on the Fracture behavior of Epoxy Nanocomposites. *J. Reinf. Plast. Compos.* **2006**, *25*, 175−188.

(47) Kosmidou, T. V.; Vatalis, A. S.; Delides, C. G.; Logakis, E.; Pissis, P.; Papanicolaou, G. C. Structural, Mechanical and Electrical Characterization of Epoxy-Amine/Carbon Black Nanocomposites. *eXPRESS Polym. Lett.* **2008**, *2*, 364−372.

(48) Fidelus, J. D.; Wiesel, E.; Gojny, F. H.; Schulte, K.; Wagner, H. D. Thermo-Mechanical Properties of Randomly Oriented Carbon/ Epoxy Nanocomposites. *Composites, Part A* **2005**, *36*, 1555−1561.

(49) Flory, P. J. Molecular Theory of Rubber Elasticity. *Polymer* **1979**, *20*, 1317−1320.

(50) Li, C.; Strachan, A. Evolution of Network Topology of Bifunctional Epoxy Thermosets During Cure and its Relationship to Thermo-Mechanical Properties: A Molecular Dynamics Study. *Polymer* **2015**, *75*, 151−160.

(51) Minoia, A.; Chen, L.; Beljonne, D.; Lazzaroni, R. Molecular Modeling Study of the Structure and Stability of Polymer/Carbon Nanotube Interfaces. *Polymer* **2012**, *53*, 5480−5490.

(52) Rittigstein, P.; Priestley, R. D.; Broadbelt, L. J.; Torkelson, J. M. Model Polymer Nanocomposites Provide an Understanding of Confinement Effects in Real Nanocomposites. *Nat. Mater.* **2007**, *6*, 278.

(53) Fryer, D. S.; Peters, R. D.; Kim, E. J.; Tomaszewski, J. E.; de Pablo, J. J.; Nealey, P. F.; White, C. C.; Wu, W.-L. Dependence of the Glass Transition Temperature of Polymer Films on Interfacial Energy and Thickness. *Macromolecules* **2001**, *34*, 5627−5634.

(54) Alcoutlabi, M.; McKenna, G. B. Effects of Confinement on Material Behaviour at the Nanometre Size Scale. *J. Phys.: Condens. Matter* **2005**, *17*, R461.

(55) Elder, R. M.; Andzelm, J. W.; Sirk, T. W. A Molecular Simulation Study of the Glass Transition of Cross-Linked Poly (Dicyclopentadiene) Networks. *Chem. Phys. Lett.* **2015**, *637*, 103−109.

(56) de Gennes, P. G. Glass Transitions in Thin Polymer Films. *Eur. Phys. J. E: Soft Matter Biol. Phys.* **2000**, *2*, 201−205.

(57) Zhu, L.; Wang, X.; Gu, Q.; Chen, W.; Sun, P.; Xue, G. Confinement-Induced Deviation of Chain Mobility and Glass Transition Temperature for Polystyrene/Au Nanoparticles. *Macromolecules* **2013**, *46*, 2292−2297.

(58) Roth, C. B.; Dutcher, J. R. Glass Transition and Chain Mobility in Thin Polymer Films. *J. Electroanal. Chem.* **2005**, *584*, 13−22.